JOURNAL OF MATERIALS SCIENCE 19 (1984) 2153–2164

The interdependence between the incidence angles associated with quasi-stable intersections during ion erosion

F. VASILIU*
National Institute for Scientific and Technical Creation, Bulev. Păcii No. 220, Sect. 6, PO Box 16, Code 79622, Bucharest, Romania

S. FRUNZĂ
Institute for Physics and Technology of Materials, PO Box MG-07, Bucharest-Magurele, R-76900, Romania

A general discussion, which is valid for any angular dependence of sputtering yield $S = S(\theta)$, concerning the interdependence between the incidence angles θ_e and θ_0, associated with quasi-stable intersections during ion erosion, is given. The object was firstly to establish the location of θ_e roots as a function of θ_0 and secondly to identify the stationary points and general trend for the complex dependence $\theta_e = \theta_e(\theta_0)$. The results obtained are applied to a quasi-stability analysis of some specific surface features during ion erosion. Various possible types of quasi-stable intersections (surface–surface, plane–surface, plane–plane) are reviewed from the point of view of their evolution caused by ion bombardment.

1. Introduction

Several earlier works [1–5] have pointed out the significance of the quasi-stable angular points evaluation in the study of mechanisms for ion-induced surface roughening, the improvement of surface analysis methods using ion beams and the applications of ion etching in microelectronics.

In a recent paper [6], a single analytical condition has been inferred, for the existence of quasi-stable angular points (having transient linear trajectories during ion erosion), relating the associated incidence angles θ_0 and θ_e only to the angular dependence of sputtering yield. This analytical condition, equivalent to the double one previously given [1, 2] and also graphically deduced on the basis of an erosion slowness curve, leads to a higher degree algebraic equation with one parameter, valid for any $S = S(\theta)$ dependence. Since $S(\theta)$ can be fitted by an algebraic polynom in $\cos\theta$ [1–4, 7–9], the algebraic equation obtained has allowed the computation of θ_e angles corresponding to a given θ_0 for three peculiar shapes of $S(\theta)$. Some angular values important for ion erosion have been estimated by similar higher degree algebraic equations [10].

This work presents a general discussion of the analytical condition stated above and implicity of the attached algebraic equation in order to establish the general character of the interdependence between the incidence angles θ_0, θ_e associated with quasi-stable intersections. The location of θ_e roots, parametrically depending on the θ_0 angle, and the identification of stationary points of $\theta_e = \theta_e(\theta_0)$ is also discussed.

2. Theoretical discussion

The similarity of $\theta_e = \theta_e(\theta_0)$ curves, where the angular values are incidence angles associated

*Present address: Institute for Physics and Technology of Materials, P.O. Box MG-07, Bucharest-Măgurele, R-76900, Romania.

0022–2461/84 $03.00 + .12

with a quasi-stable intersection (angular point) during ion erosion [6] has suggested a general discussion on θ_e roots as a function of θ_0. For the existence of a quasi-stable surface–surface, plane–surface or plane–plane intersection, the angles θ_e and θ_0 must satisfy the previously inferred analytical condition:

$$\left.\frac{dS}{d\theta}\right|_{\theta=\theta_e} = \frac{\cos\theta_0\,[S(\theta_0)-S(\theta_e)]}{\cos\theta_e \sin(\theta_0-\theta_e)} \qquad (1)$$

In the following discussion the following notation will be used:

$$F(\theta_e,\theta_0) = \left.\frac{dS}{d\theta}\right|_{\theta=\theta_e} - \frac{\cos\theta_0\,[S(\theta_0)-S(\theta_e)]}{\cos\theta_e \sin(\theta_0-\theta_e)} \qquad (2)$$

In the angular range $\theta_e \in [-90°, +90°]$, we shall consider six (a, b) intervals: $(-90°, -\theta_{s_2})$, $(-\theta_{s_2}, -\theta_{s_1})$, $(-\theta_{s_1}, 0°)$, $(0°, \theta_{s_1})$, $(\theta_{s_1}, \theta_{s_2})$ and $(\theta_{s_2}, 90°)$, where $-\theta_{s_2}$, $-\theta_{s_1}$, $+\theta_{s_1}$, $+\theta_{s_2}$ are the consecutive roots of the derivative $dF/d\theta_e$.

It is well known that there is no θ_e root in the range (a, b) if $F(a, \theta_0)F(b, \theta_0) \geqslant 0$ and at the most one root θ_e if $F(a, \theta_0)F(b, \theta_0) < 0$, for a given θ_0 value.

In order to locate the θ_e roots depending on θ_0, the variation of the sign for $F(\theta_e, \theta_0)$ is presented in Table I, taking into account the sign of each term in Equation 2, easily established as follows:

$$\left.\frac{dS}{d\theta}\right|_{\theta=\theta_e} \begin{cases} > 0 \text{ for } \theta_e \in [-90°, -\theta_p) \cup (0°, \theta_p) \\ 0 \text{ for } \theta_e = 0° \text{ and } \theta_e = \mp\theta_p \\ < 0 \text{ for } \theta_e \in (-\theta_p, 0°) \cup (\theta_p, 90°] \end{cases} \qquad (4)$$

$$\sin(\theta_0-\theta_e) \begin{cases} > 0 \text{ for } \theta_e \in [-90°, \theta_0) \\ 0 \text{ for } \theta_e = \theta_0 \\ < 0 \text{ for } \theta_e \in (\theta_0, 90°] \end{cases} \qquad (5)$$

$$S(\theta_0)-S(\theta_e) \begin{cases} 0 \text{ for } \theta_e \in [-90°, -\hat{\theta}_0) \cup (-\theta_0, \theta_0) \cup (\hat{\theta}_0, 90°] \\ 0 \text{ for } \theta_e = \pm\theta_0, \pm\hat{\theta}_0 \\ < 0 \text{ for } \theta_e \in (-\hat{\theta}_0, -\theta_0) \cup (\theta_0, \hat{\theta}_0) \end{cases} \qquad (6)$$

The discussion will involve the location of the roots θ_e of the equation $F(\theta_e, \theta_0) = 0$ as a function of θ_0, the identification of stationary points and the determination of the general variation trend of the complex $\theta_e = \theta_e(\theta_0)$ dependence.

2.1. Roots location

The θ_e roots of the equation $F(\theta_e, \theta_0) = 0$, also satisfying the Condition 1, are placed between the roots of the derivative $dF/d\theta_e$, which can be easily written as:

$$\frac{dF}{d\theta_e} = \left.\frac{d^2S}{d\theta^2}\right|_{\theta=\theta_e} - 2\tan\theta_e \left.\frac{dS}{d\theta}\right|_{\theta=\theta_e} \qquad (3)$$

The equation $dF/d\theta_e = 0$ has four roots; $\pm\theta_{s_1}$, $\pm\theta_{s_2}$, known as the inflexion points of the erosion slowness curve [2, 3]. The same angles, θ_s, are associated with the returning points having an unique tangent on the cursor-shaped polar diagram representing $V(\theta)/V(0°)$ plotted against recession angle ψ [2].

(in Condition 6 the angle $\hat{\theta}_0$ satisfies the equation $S(\theta_0) = S(\hat{\theta}_0)$).

The last sign in Condition 6 is valid for $0° < \theta_0 < \theta_p$ and is also true for $\theta_p < \theta_0 < 90°$ if $\theta_0 \neq \hat{\theta}_0$.

In Table I, the location of θ_e roots is indicated as a function of θ_0. The angles $\pm\theta_p$ and $\pm\theta_0^*$ (where $S(\theta_0^*) = S(0°)$) are also included for a more precise location. Although an extensive discussion will be made in Section 2.3, the variation in trend of θ_e roots depending on θ_0 is roughly marked in the table.

Taking into account the symmetry properties of the function $F(\theta_e, \theta_0)$, in Table I only the θ_e root location for $\theta_0 \in [0°, 90°]$ is given because for $\theta_0 \in [-90°, 0°]$ the behaviour is similar. For example, the location of θ_e roots ($\theta_e \in [-90°, 0°]$ and $[0°, 90°]$) as a function of θ_0 parameter ($\theta_0 \in [-90°, 0°]$) is identical to that of θ_e roots placed for $\theta_0 \in [0°, 90°]$ in the range $\theta_e \in [0°, 90°]$ and $[-90°, 0°]$ respectively. These symmetry proper-

TABLE I The sign variation of the function $F(\theta_e, \theta_0)$

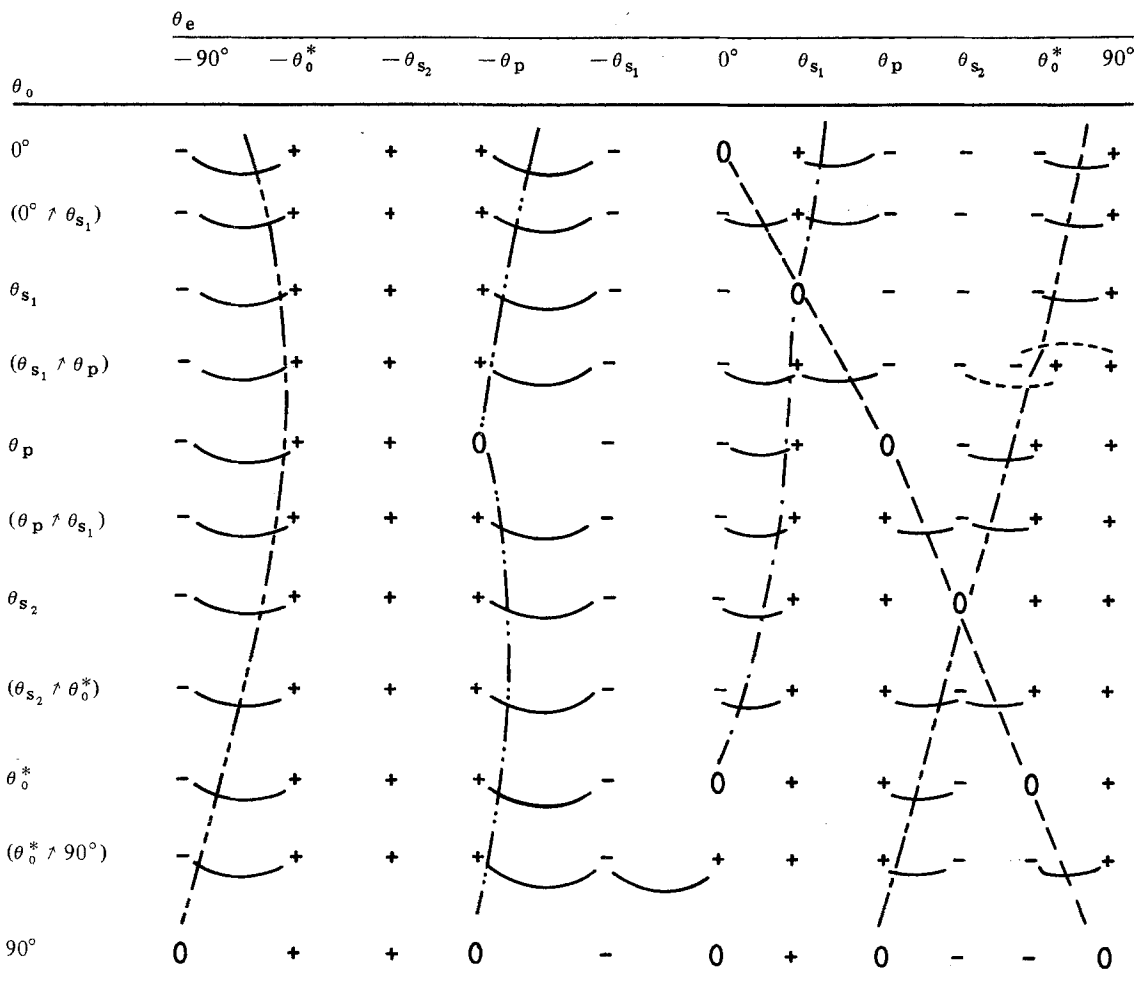

Location of roots

- - - - $\theta^0_{e_1} = \theta_0$ (physically trivial solution)
-·-·-·- $\theta^1_{e_1} > 0°$ (except for $\theta_0 \in (\theta_0^*, 90°)$ where $\theta^1_{e_1} < 0°$ if $\theta^1_{e_1}$ exists, being marked by . . . . .)
------- $\theta^2_{e_1} > 0°$
-··-··-·· $\theta^1_{e_2} < 0°$
------- $\theta^2_{e_2} < 0°$

ties as opposed to the point $\theta_0 = \theta_e = 0°$ of the dependence $\theta_e = \theta_e(\theta_0)$, connected to the possible interchange of the incidence angles θ_0 and θ_e, have been proved and numerically exemplified in some peculiar cases in a previous work [6].

Generally, the equation $F(\theta_e, \theta_0) = 0$ has four θ_e roots: $\theta^1_{e_1}$, $\theta^2_{e_1}$ (positive) and $\theta^1_{e_2}$, $\theta^2_{e_2}$ (negative), for $\theta_0 \in [0^b, 90°]$, except for the physically trivial solution $\theta^0_{e_1} = \theta_0$ which corresponds to the lack of angular points. However, for the dependences $S = S(\theta)$ which rapidly increase at small θ angles, an extension of the branch $\theta^1_{e_1}$ having negative values could be obtained for $\theta_0 \in (\theta_0^*, 90°)$. In this last case, the above equation will have one positive and three negative roots. For $\theta_0 = \theta_0^*$, the solutions will be: $\theta^1_{e_1} = 0°, \theta^2_{e_1} > 0°$ and $\theta^1_{e_2}, \theta^2_{e_2} < 0°$.

To clarify the discussion concerning θ_e roots location as a function of θ_0, the curves $\theta_e = \theta_e(\theta_0)$ for a hypothetical $S = S(\theta)$ dependence are plotted in Fig. 1. They are similar to those obtained for the specified $S = S(\theta)$ [6]. The branches noted, θ^1_e and θ^2_e, are obtained by connecting the segments $\theta^1_{e_1}, \theta^1_{e_2}$ and $\theta^2_{e_1}, \theta^2_{e_2}$, respectively.

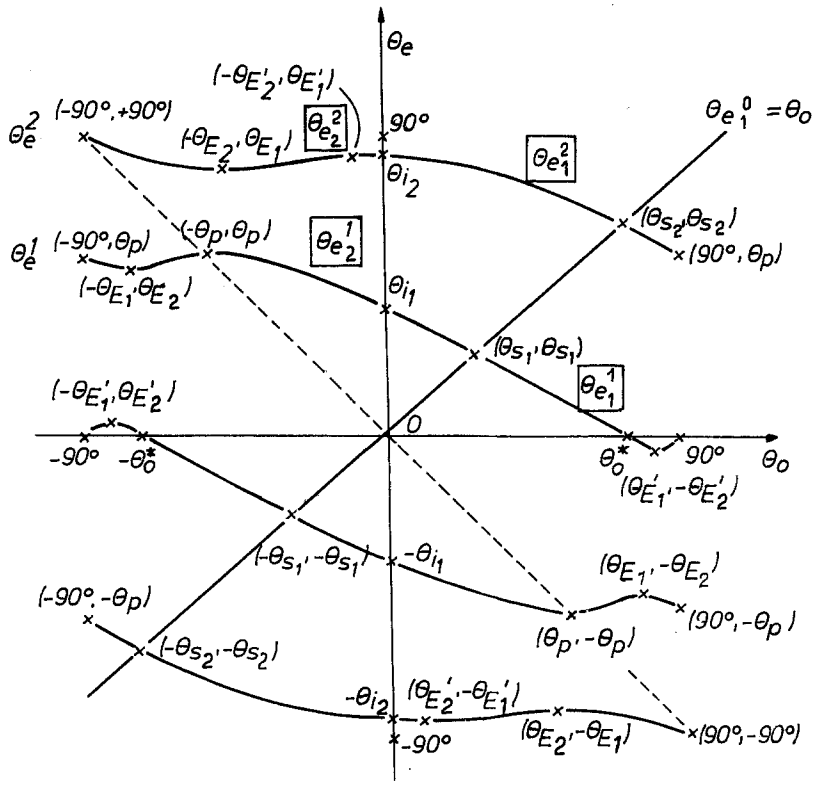

Figure 1 The dependence $\theta_e = \theta_e(\theta_o)$ calculated as described in [6] for a hypothetical angular variation of sputtering yield $S = S(\theta)$.

Table II presents the summary of the θ_e roots location depending on θ_0. θ_e roots are placed in certain intervals, their variation trend as a function of increasing θ_0 being indicated by arrows. The results are also confirmed in Sections 2.2 and 2.3 by the study of the function $F(\theta_e, \theta_0)$.

Discussion of Tables I and II is generalized for any $S = S(\theta)$ function which fits the experimentally observed angular variation of sputtering yield. The numerical results obtained for three $S = S(\theta)$ functions [6] correspond to this general discussion. The same conclusions could be graphically deduced by using the cursor-shaped polar diagram $V(\theta)/V(0°)$ plotted against angle ψ [2] as was previously reported [6, 11].

If $S = S(\theta)$ has such a form that the equation:

$$\sin\theta \cos\theta \frac{dS}{d\theta} - S(\theta) = 0 \qquad (7)$$

TABLE II The location of θ_e roots as function of θ_0

$\theta_0 = \theta_{e_1}^1$	$\theta_{e_1}^1$	$\theta_{e_1}^2$	$\theta_{e_2}^1$	$\theta_{e_2}^2$
$0°$	$\theta_i^1 \in (\theta_{s_1}, \theta_p)$	$\theta_i^2 \in (\theta_o^*, 90°)$	$-\theta_i^1 \in (-\theta_p, -\theta_{s_1})$	$-\theta_i^2 \in (-90°, -\theta_o^*)$
$0° \uparrow \theta_0 \uparrow \theta_{s_1}$	$(\theta_{s_1} \downarrow \theta_p)$	$(\theta_o^* \downarrow 90°)$	$(-\theta_p \downarrow -\theta_{s_1})$	$(-90° \uparrow -\theta_o^*)$
θ_{s_1}	θ_{s_1}	$(\theta_o^*, 90°)$	$(-\theta_p, -\theta_{s_1})$	$(-90°, -\theta_o^*)$
$\theta_{s_1} \uparrow \theta_0 \uparrow \theta_p$	$(0° \downarrow \theta_{s_1})$	$(\theta_o^* \downarrow 90°)$ or $(\theta_{s_2} \downarrow \theta_o^*)$	$(-\theta_p \downarrow -\theta_{s_1})$	$(-90° \uparrow\downarrow -\theta_o^*)$
θ_p	$(0°, \theta_{s_1})$	$(\theta_{s_1}, \theta_o^*)$	$-\theta_p$	$(-90°, -\theta_o^*)$
$\theta_p \uparrow \theta_0 \uparrow \theta_{s_2}$	$(0° \downarrow \theta_{s_1})$	$(\theta_{s_2} \downarrow \theta_o^*)$	$(-\theta_p \uparrow -\theta_{s_1})$	$(-90°, \downarrow -\theta_o^*)$
θ_{s_2}	$(0°, \theta_{s_1})$	θ_{s_2}	$(-\theta_p, -\theta_{s_1})$	$(-90°, -\theta_o^*)$
$\theta_{s_2} \uparrow \theta_0 \uparrow \theta_o^*$	$(0° \downarrow \theta_{s_1})$	$(\theta_p \downarrow \theta_{s_2})$	$(-\theta_p \uparrow -\theta_{s_1})$	$(-90° \downarrow -\theta_o^*)$
θ_o^*	$0°$	(θ_p, θ_{s_2})	$(-\theta_p, -\theta_{s_1})$	$(-90°, -\theta_o^*)$
$\theta_o^* \uparrow \theta_0 \uparrow 90°$	$(-\theta_{s_1} \downarrow \uparrow 0°)$	$(\theta_p \downarrow \theta_{s_1})$	$(-\theta_p \uparrow\downarrow -\theta_{s_1})$	$(-90° \downarrow -\theta_o^*)$
$90°$	$0°$	θ_p	$-\theta_p$	$-90°$

has two solutions θ_{t_1}, θ_{t_2} [10], then the θ_e roots could be more closely localized by considering the angular values θ_t and $\hat{\theta}_t$ ($S(\theta_t) = S(\hat{\theta}_t)$).

Finally, it is important to observe from Table I the occurrence of the domains (θ_0, θ_e) in which the function F has an unique sign, the θ_e solutions of the equation $F(\theta_e, \theta_0) = 0$ being the boundaries of these domains. The sign changes can also be revealed at the boundary crossing by means of the sign of derivative F'_{θ_e} which has the roots $\pm \theta_{s_1}$, $\pm \theta_{s_2}$ [2, 3]. In fact, since $F'_{\theta_e} > 0$ for any given θ_0 in the ranges $\theta_e \in (-90°, -\theta_{s_2}) \cup (0°, \theta_{s_1}) \cup (\theta_{s_2}, 90°)$, the function F is increasing. Thus, the crossing of the boundaries $\theta^2_{e_2}$; $\theta^0_{e_1} = \theta_0$, $\theta^1_{e_1}$ and $\theta^2_{e_1}$, $\theta^0_{e_1} = \theta_0$, respectively, takes place from negative to positive values for increasing θ_e in the ranges given (see Table I). For $\theta_e \in (-\theta_{s_2}, \theta_{s_1}) \cup (\theta_{s_1}, \theta_{s_2})$ we have $F'_{\theta_e} < 0$ so that the function F decreases which also implies the crossing of boundaries $\theta^1_{e_2}$ and $\theta^1_{e_1}$, $\theta^0_{e_1} = \theta_0$, $\theta^2_{e_1}$, respectively, from the positive to the negative values.

2.2. Identification of stationary points

The stationary points of the dependences $\theta_e = \theta_e(\theta_0)$ will be determined using Equation 3. Since the equation $F(\theta_e, \theta_0) = 0$ contains implicitly the dependence $\theta_e = \theta_e(\theta_0)$, a well known theorem leads to the following result:

$$\frac{d\theta_e}{d\theta_0} = -\frac{F'_{\theta_0}}{F'_{\theta_e}} \tag{8}$$

By taking the derivative of function F against θ_0 and by using Equation 1, equivalent to $F = 0$, we obtain:

$$\frac{dF}{d\theta_0} = \frac{\cos^2\theta_e \left.\frac{dS}{d\theta}\right|_{\theta=\theta_e} - \cos^2\theta_0 \left.\frac{dS}{d\theta}\right|_{\theta=\theta_0}}{\cos\theta_0 \cos\theta_e \sin(\theta_0 - \theta_e)} \tag{9}$$

Therefore, by substituting F'_{θ_e} and F'_{θ_0} from Equations 3 and 9, respectively, Equation 8 becomes:

$$\frac{d\theta_e}{d\theta_0} = \frac{\cos^2\theta_0 \left.\frac{dS}{d\theta}\right|_{\theta=\theta_0} - \cos^2\theta_e \left.\frac{dS}{d\theta}\right|_{\theta=\theta_e}}{\cos\theta_0 \cos\theta_e \sin(\theta_0 - \theta_e)\left[\left.\frac{d^2S}{d\theta^2}\right|_{\theta=\theta_e} - 2\tan\theta_e \left.\frac{dS}{d\theta}\right|_{\theta=\theta_e}\right]} \tag{10}$$

The stationary points of the multi-shaped dependence $\theta_e = \theta_e(\theta_0)$ are the roots of the equation $d\theta_e/d\theta_0 = 0$, which leads to:

$$\cos^2\theta_0 \left.\frac{dS}{d\theta}\right|_{\theta=\theta_0} - \cos^2\theta_e \left.\frac{dS}{d\theta}\right|_{\theta=\theta_e} = 0 \tag{11}$$

Later the extremum points of the dependence $\theta_e = \theta_e(\theta_0)$ will be specified, taking into account the physical meaning in each case. The type of each extremum point will be later established in Section 2.3 by the study of derivative $d\theta_e/d\theta_0$. Some stationary points have been identified by numerical computation for specific $S = S(\theta)$ curves [6], although their existence has not been mathematically demonstrated for any function $S = S(\theta)$ proper to describe the angular variation of sputtering yield.

The extremum Condition 11 leads to the following (θ_0, θ_e) stationary points, marked in Fig. 1, except for the trivial solution $\theta_e = \theta_0$ which corresponds to the lack of angular points:

(a) $\theta_0 = \mp 90°$, $\theta_e = \pm 90°$ is a marginal absolute extremum of $\theta^2_e = \theta^2_e(\theta_0)$ (maximum for $\theta_e > 0°$, minimum for $\theta_e < 0°$). Physically, this case corresponds to the grazing bombardment of a vertical wall with a vanishing thickness;

(b) $\theta_0 = \mp 90°$, $\theta_e = \pm \theta_p$ signifies a marginal extremum point of the dependence $\theta^1_e = \theta^1_e(\theta_0)$ (maximum for $\theta_e > 0°$, minimum for $\theta_e < 0°$). This point is connected to the bombardment of an acute angle $(90° - \theta_p)$ edge with an ion beam perfectly grazing to one microfacet. It is evident that the regression trajectory of the angular point will be along the microfacet grazingly oriented to the ion beam;

(c) $\theta_0 = \mp \theta_p$, $\theta_e = \pm \theta_p$ corresponds to the absolute extremum point of the dependence $\theta^1_e = \theta^1_e(\theta_0)$ (maximum for $\theta_e > 0°$, minimum for $\theta_e < 0°$). This important case is related to the bombardment of an edge (acute angle $180° - 2\theta_p$) along its bisector, the microfacet normals making a θ_p angle with the ion-beam direction. The angular point regression will take place along the edge symmetry axis coinciding with the beam direction. Stable plane–plane intersections of this type have already been mentioned by Carter *et al.* [2, 11].

(d) $\theta_0 = \pm 90°$, $\theta_e = \pm \theta_p$ is an absolute and

TABLE III Discussion of the dependence $\theta_e^1 = \theta_e^1(\theta_0)$

θ_0	$-90°$	↑	$-\theta_{E_1}$	↑	$-\theta_p$	↑	$0°$	↑	θ_{s_1}	↑	θ_p	↑	θ_0^*	↑	θ'_{E_1}	↑	$90°$
θ_e^1	θ_p		θ_{E_2}		θ_p		θ_{i_1}		θ_{s_1}				$0°$		$-\theta'_{E_2}$		$0°$
$\sin(\theta_0 - \theta_e^1)$	−	−	−	−	−	−	−	−	0	+	+	+	+	+	+	+	+
$\left.\frac{d^2S}{d\theta^2}\right\|_{\theta=\theta_e^1} - 2\tan\theta_e^1 \left.\frac{dS}{d\theta}\right\|_{\theta=\theta_e^1}$	−	−	−	−	−	−	−	−	0	+	+	+	+	+	+	+	+
$\cos^2\theta_0 \left.\frac{dS}{d\theta}\right\|_{\theta=\theta_0}$	0	+	+	+	0	−	0	+	+	+	0	−	−	−	−	−	0
$\cos^2\theta_e^1 \left.\frac{dS}{d\theta}\right\|_{\theta=\theta_e^1}$	0	+	+	+	0	+	+	+	+	+	+	+	0	−	−	−	0
$\cos^2\theta_0 \left.\frac{dS}{d\theta}\right\|_{\theta=\theta_0} - \cos^2\theta_e^1 \left.\frac{dS}{d\theta}\right\|_{\theta=\theta_e^1}$	0	−	0	+	0	−	−	−	0	−	−	−	−	−	0	+	0
$\frac{d\theta_e^1}{d\theta_0}$	0	−	0	+	0	−	−	−	1	−	−	−	−	−	0	+	0
θ_e^1	$\frac{\theta_p}{M_1}$	↓	$\frac{\theta_{E_2}}{m_1}$	↑	$\frac{\theta_p}{M_a}$	↓	θ_{i_1}	↓	θ_{s_1}	↓	↓	↓	$0°$	↓	$\frac{\theta'_{E_2}}{m_a}$	↑	$\frac{0°}{M_1}$

marginal stationary point of the dependence $\theta_e^2 = \theta_e^2(\theta_0)$ (minimum for $\theta_e > 0°$, maximum for $\theta_e < 0°$). Unlike case (b), the physical meaning consists here of the bombardment of an abtuse angle $(90° + \theta_p)$ edge with an ion beam perfectly grazing one of the microfacets:

(e) $\theta_0 = \pm 90°$, $\theta_e = 0°$ corresponds to a marginal extremum point of the dependence $\theta_e^1 = \theta_e^1(\theta_0)$ (minimum for $\theta_0 < 0°$, maximum for $\theta_0 > 0°$), physically connected to the grazing irradiation along one face of a normal intersection. The regression of angular points takes place along the same face;

(f) other extremum points (θ_0, θ_e) can be obtained by solving the system of Equations 1 and 11. These stationary points, denoted θ_E by Carter *et al.* [2], are connected to some stable plane–plane intersections, also graphically identified on the associated polar diagrams [6, 10]. In Fig. 1, these stationary points are marked as follows:

(i) $-\theta_0 = \pm \theta_{E_1}$, $\theta_e = \mp \theta_{E_2}$ (local extremum for $\theta_e^1 = \theta_e^1(\theta_0)$ – maximum for $\theta_e < 0°$, minimum for $\theta_e > 0°$)

(ii) $-\theta_0 = \pm \theta_{E_2}$, $\theta_e = \mp \theta_{E_1}$ (local extremum for $\theta_e^2 = \theta_e^2(\theta_0)$ – maximum for $\theta_e < 0°$, minimum for $\theta_e > 0°$)

(iii) $-\theta_0 = \pm \theta'_{E_1}$, $\theta_e = \mp \theta'_{E_2}$ (absolute extremum for $\theta_e^1 = \theta_e^1(\theta_0)$ – minimum for $\theta_e < 0°$, maximum for $\theta_e > 0°$).

(iv) $-\theta_0 = \mp \theta'_{E_2}$, $\theta_e = \pm \theta'_{E_1}$ (local extremum for $\theta_e^2 = \theta_e^2(\theta_0)$ – minimum for $\theta_e < 0°$, maximum for $\theta_e > 0°$).

Although the stationary points θ'_E have not been identified on the curves $\theta_e = \theta_e(\theta_0)$ numerically calculated for some specific $S = S(\theta)$ dependences [6], they could appear for rapidly increasing angular variation of sputtering yield at small angles.

The values $\theta_{E_1}, \theta_{E_2}$ correspond to the ir location on the erosion slowness curve given by Carter *et al.* [2]: $\theta_{E_1} \in (\theta_{s_2}, 90°)$, $\theta_{E_2} \in (\theta_{s_1}, \theta_{s_2})$. As has resulted from previously given graphical evaluations [6, 10], these values can be more closely localized: $\theta_{E_1} \in (\theta_{s_2}, \theta^*_{i_2})$ and $\theta_{E_2} \in (\theta^*_{i_1}, \theta_p)$. In the same manner, $\theta'_{E_1} \in (\theta^*_{i_2}, 90°)$ and $\theta'_{E_2} \in (0°, \theta_{s_1})$.

2.3. Variation trend of $\theta_e = \theta_e(\theta_0)$ dependences

The variation trend of $\theta_e^1 = \theta_e^1(\theta_0)$ and $\theta_e^2 = \theta_e^2(\theta_0)$ curves (Fig. 1) can be easy established using the derivative sign inferred from Equation 10. Both the sign of the derivative and the variation trend for each of the two curves are given in Tables III and IV, respectively.

Table III confirms the known variation trend of $\theta_e^1 = \theta_e^1(\theta_0)$ and the already mentioned stationary points: one absolute maximum ($\theta_0 = -\theta_p$, $\theta_e^1 = \theta_p$), two local maxima at range ends

TABLE IV The dependence $\theta_e^2 = \theta_e^2(\theta_0)$

θ_0	$-90°$	↑	$-\theta_p$	↑	$-\theta_{E_2}$	↑	$-\theta'_{E_2}$	↑	$0°$	↑	θ_p	↑	θ_{s_2}	↑	$90°$
θ_e^2	$90°$		θ_{E_1}		θ'_{E_1}		θ_{i_2}						θ_{s_2}		θ_p
$\sin(\theta_0 - \theta_e^2)$	0	−	−	−	−	−	−	−	−	−	−	−	0	+	+
$\left.\frac{d^2S}{d\theta^2}\right\|_{\theta=\theta_e^2} - 2\tan\theta_e^2 \left.\frac{dS}{d\theta}\right\|_{\theta=\theta_e^2}$	+	+	+	+	+	+	+	+	+	+	+	+	0	−	−
$\cos^2\theta_0 \left.\frac{dS}{d\theta}\right\|_{\theta=\theta_0}$	0	+	0	−	−	−	−	−	0	+	0	−	−	−	−
$\cos^2\theta_0 \left.\frac{dS}{d\theta}\right\|_{\theta=\theta_0} - \cos^2\theta_e^2 \left.\frac{dS}{d\theta}\right\|_{\theta=\theta_e^2}$	0	+	+	+	0	−	0	+	+	+	+	+	+	+	0
$\frac{d\theta_e^2}{d\theta_0}$	0	−	−	−	0	+	0	-	−	−	−	−	1	−	0
θ_e^2	$\frac{90°}{M_a}$	↓	↓	↓	$\frac{\theta_{E_1}}{m_i}$	↑	$\frac{\theta'_{E_1}}{M_i}$	↓	θ_{i_2}	↓	↓	↓	θ_{s_2}	↓	$\frac{\theta_p}{m_a}$

($\theta_0 = -90°$, $\theta_e^1 = \theta_p$ and $\theta_0 = 90°$, $\theta_e^1 = 0°$), one absolute minimum ($\theta_0 = \theta'_{E_1}$, $\theta_e^1 = -\theta'_{E_2}$) and one local minimum ($\theta_0 = -\theta_{E_1}$, $\theta_e^1 = \theta_{E_2}$) (Fig. 1.).

According to Table IV, the dependence $\theta_e^2 = \theta_e^2(\theta_0)$ has one marginal absolute maximum ($\theta_0 = -90°$, $\theta_e^2 = 90°$), one local maximum ($\theta_0 = -\theta'_{E_2}$, $\theta_e^2 = \theta'_{E_1}$), one marginal absolute minimum ($\theta_0 = 90°$, $\theta_e^2 = \theta_p$) and one local minimum ($\theta_0 = -\theta'_{E_2}$, $\theta_e^2 = \theta'_{E_1}$) (Fig. 1).

3. Applications of the theory

The analytical Equation 1 for the existence of the quasi-stable angular points, having a linear trajectory during ion erosion, implies that any surface intersection, characterized by θ_0, θ_e incidence angles connected by Equation 1, remains stable if no interference appears with other adjacent angular points during their recessive motion.

The above discussion has allowed an analysis of the interdependence between incidence angles θ_0 and θ_e associated with quasi-stable intersections during ion erosion. Various possible types of quasi-stable intersections will be reviewed later from the point of view of their evolution caused by ion bombardment.

There are only a few orientations (θ_0, θ_e) associated with quasi-stable angular points for plane–plane intersections and they coincide with the stationary points of the dependence $\theta_e = \theta_e(\theta_0)$, which is generally characteristic for surface–surface or plane–surface intersections. The extremum Condition 11 and the analytical Condition 1 evidently require not only identical motion directions and velocities for intersection edge and microfacets but also a unique linear trajectory of intersection. The system of both these conditions has the following solutions:

$$\theta_0 = \pm\theta_p,\ \theta_e = \mp\theta_p$$
$$\theta_0 = \pm 90°,\ \theta_e = \mp\theta_p$$
$$\theta_0 = \pm 90°,\ \theta_e = \pm\theta_p$$
$$\theta_0 = 0°,\ \theta_e = \pm 90°$$
$$\theta_0 = \pm\theta_{E_1},\ \theta_e = \mp\theta_{E_2}$$
$$\theta_0 = \pm\theta_{E_2},\ \theta_e = \mp\theta_{E_1}$$
$$\theta_0 = \pm\theta'_{E_1},\ \theta_e = \mp\theta'_{E_2}$$
$$\theta_0 = \pm\theta'_{E_2},\ \theta_e = \mp\theta'_{E_1}$$

Previous theoretical and experimental results [2, 11–25] have established that many of the above orientations lead to quasi-stable plane–plane intersections. In the framework of the present discussion, the quasi-stability analysis of some specific topographic shapes already studied can be valuable.

Many works [1–3, 11–21, 25] have pointed out the relative stability of conical shapes bombarded along their axis and having as top angle $\alpha = 180° - 2\theta_p$. The quasi-stable intersection of two surfaces (planes) making with an ion beam the incidence angles $\theta_0 = \pm\theta_p$, $\theta_e = \mp\theta_p$ contains the experimentally observed case of ridges or cones aligned along a random direction of ion beam at angle θ_p to the respective normals. However, these cones or ridges lying on a horizontal plane are only metastable shapes due to the evolution of basis contact points leading finally to a tail whose appearance has been recently explained [11].

The topographic shapes of ridge, pyramidal or conical type, having θ^* as basis angles and $\pi - 2\theta^*$ as top angle, have been initially considered as stable [7]. According to the previous computer simulations [3, 8], the present work proves that this statement is not correct, since the top edge is not a quasi-stable plane–plane intersection even if the basis contact points are quasi-stable.

It has been shown experimentally and theoretically [2, 25–28] that isolated ridges, pyramids or cones lying on a horizontal surface are generally unstable and transient at normal and oblique incidence ion bombardment. In fact, our results confirm the instability of these ion-eroded cones or pyramids, leading to considerable topographical modifications. Thus, some pre-existing angular points are not stable and unique during the evolution of surface topography. For example, the basis contact points for a half angle of $(\pi/2) - \theta_p$ (Fig. 2a) and the top point for a half angle of $(\pi/2) - \theta^*$ (Fig. 2b) are unstable, as has already been mentioned, since new angular points are generated from those pre-existing.

The stable cones formed in a pit having vertical side walls frequently observed in ion bombardment experiments [29, 30] correspond to a stable combination of orientations (0°, ± 90°), (+ 90°, $\mp\theta_p$) and ($\pm\theta_p$, $\mp\theta_p$) (Fig. 3a).

According to our results, the dense arrays of cones or pyramids whose microfacet normals make, with the ion beam direction, such angles as:

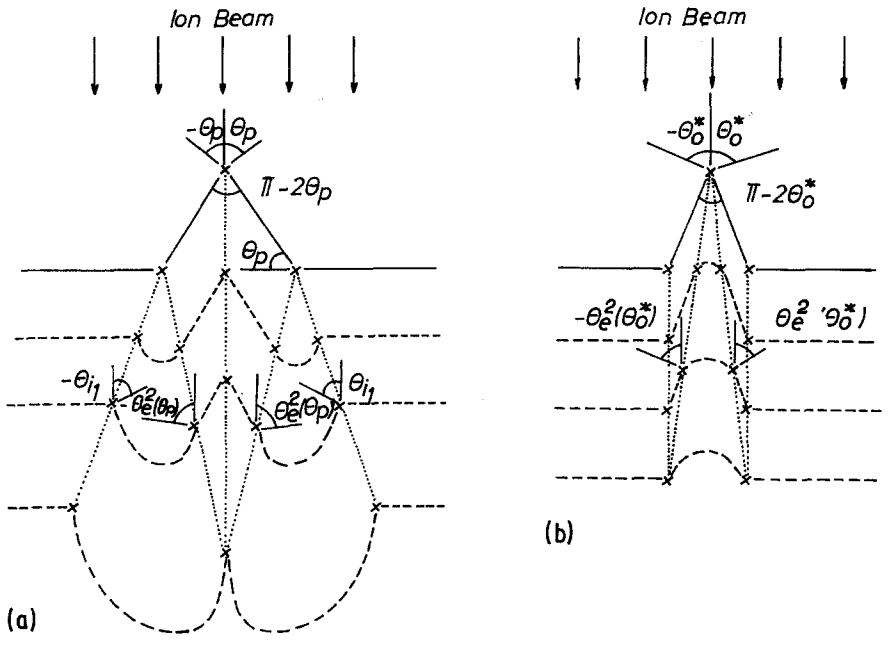

Figure 2 The evolution of unstable angular points during ion erosion characteristics for conical (pyramidal) features: (a) half angle $\alpha = (\pi/2) - \theta_p$; (b) half angle $\alpha = (\pi/2) - \theta^*$.

(1) $(\pm\theta_p, \mp\theta_p)$ – normal incidence (Fig. 3b), (2) $(\pm\theta_{E_1}, \mp\theta_{E_2})$, and (3) $(\pm\theta'_{E_1}, \mp\theta'_{E_2})$ – normal and oblique incidence (Figs. 3c to f) should present a persistent stability. Recently, the stability of cone or pyramid forests, formed on some monocrystalline surfaces of special orientation at normal and oblique ion incidence [29, 31, 32] has been discussed [27] but it was not possible to distinguish whether the stability is due to the continuous generation of new features or whether these arrays are really stable. The orientations mentioned above correspond in our opinion to a true stability. If the top angles of conical (pyramidal) microtopography are not equal to $\pi - 2\theta_p$, $\pi - \theta_{E_1} - \theta_{E_2}$, $\pi - \theta'_{E_1} - \theta'_{E_2}$, respectively, and/or the surface covering is not complete, it is possible that the angular point evolution results in feature shrinking and disappearance.

The combination of horizontal and vertical surfaces, eventually forming "honeycomb" structures, has been considered as a stable feature at normal ion bombardment [2, 12]. This topography corresponds physically to the stability case: $(\theta_0 = 0°, \theta_e = \pm 90°)$ (Fig. 3g).

"Pillar" structures consisting of a cone of top angle $\pi - 2\theta_p$ superimposed on a vertical cylinder have been identified as very stable at normal ion irradiation on stainless steel surfaces [20]. This case is related to a combination of theoretically stable orientations: $(\pm\theta_p, \mp\theta_p)$, $(\pm 90°, \pm\theta_p)$ and $(0°, \pm 90°)$ (Fig. 3b).

Various structures of high stability such as cliff [33, 34] or terraced [26, 35, 36] ones can be connected to stable orientation pairs: $(0°, \pm\theta_{i_1})$; $(0°, \pm\theta_{i_2})$ and $(0°, \pm\theta_0^*)$ (Figs. 3i, j).

Besides the experimental cases mentioned, there could be conceived a great number of topographical shapes having high theoretical stability during ion bombardment. "Mesas" and "plateaux" having slide slopes inclined at θ_{i_1}, $\theta_0{}^*$, θ_{i_2} ($\theta_{i_1} \approx \theta_p$; θ_0^*, $\theta_{i_2} \approx 90°$) and lying directly on the horizontal surface (Fig. 3k) or superimposed on a vertical cylinder or prism (Fig. 3l) are such cases. Some experimental observations of protuberant features of "mesa" or "plateau" type [30, 37, 38] appear to be in accordance with the above considerations.

In Figs. 3b to f, h, k, and l are also shown, for different stability cases, both symmetric profiles, representing "mirror" images as opposed to a virtual horizontal surface.

The agreement of the previous experimental data with the theoretical results given here suggests a possible distinction between three types of quasi-stable intersections, from the point of view of their specific evolution:

(a) surface–surface, plane–surface or plane–

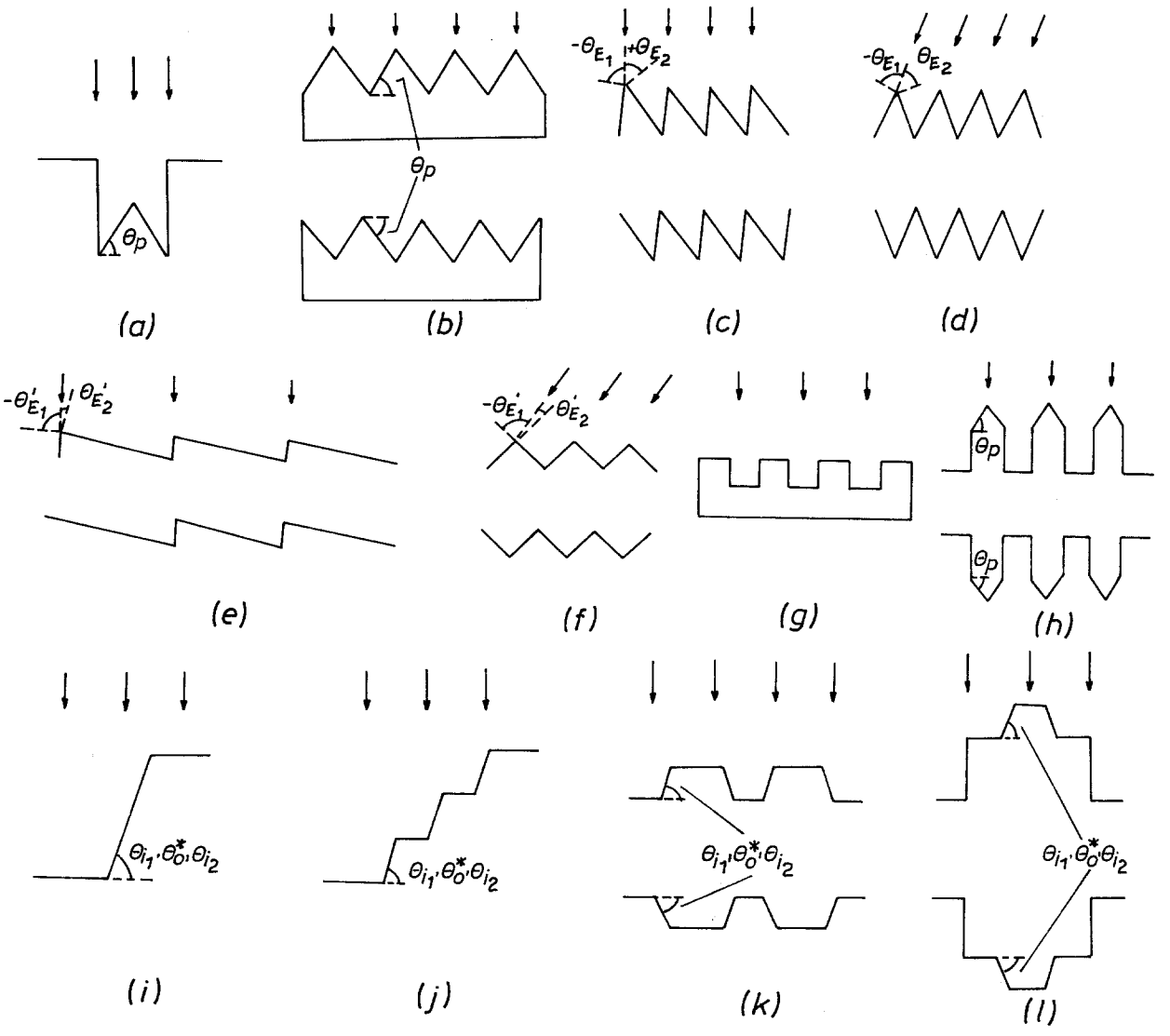

Figure 3 Specific topographic features or microreliefs showing a combination of quasi-stable angular points. During ion bombardment at normal or oblique incidence a transient or persistent stability can occur as function of trajectory interference effects.

plane intersections characterized by random orientations (θ_0^1, θ_0^2) which do not satisfy the analytical Equation 1. According to earlier works [1–3, 39] each of these original edges will produce, during ion erosion, two or more other new quasi-stable angular points having different linear trajectories and being associated to the orientations $(\theta_0^1, \theta_e(\theta_0^1))$ and $(\theta_0^2, \theta_e(\theta_0^2))$, respectively. A new curved microfacet, connected with the surface (planes) forming the initial intersection, might develop between the two trajectories. Finally, a local instantaneous change of the original microprofile is expected. This general case corresponds to the results of Ducommun *et al.* [1] and Cantagrel [39] concerning the evolution of eroded steps in silicon. The numerical values given in these works are in very good agreement with those algebraically estimated in the framework of the present approach [6, 10];

(b) Surface–surface or plane–surface intersections characterized by special orientations $(\theta_0, \theta_e(\theta_0))$ where the incidence angles θ_0, θ_e satisfy the analytical quasi-stability condition for angular points given in [6] and discussed in the present work;

(c) plane–plane intersections characterized by very restricted (θ_0, θ_e) orientation pairs, coinciding with the stationary points of the $\theta_e = \theta_e(\theta_0)$

dependence. Many earlier works [2, 11–25] were concerned about various quasi-stable plane–plane intersections of this type.

In the last two special cases, the intersections could temporarily remain unique and stable until their trajectories interfere with the trajectories or other adjacent angular points upon the eroded microprofile. Although their character is practically transient, these intersections are translated on a single linear trajectory in the range of their time stability. Thus, a possible relation between the initial and ion-eroded surface microtopography can be established by means of these quasi-stable edges at least until drastic relief modifications appear due to the subsequent intersections of close angular point trajectories.

A true stability during ion erosion could be obtained for special microprofiles exclusively containing quasi-stable intersections of b and c type, arranged so that no adjacent interference effects occur. Thus, the initial microprofiles of this kind would be infinitely reproduced during ion bombardment.

4. Conclusions

The interdependence between the incidence angles θ_0 and θ_e associated to quasi-stable intersections during ion erosion has been discussed. This has allowed the location of θ_e roots as function of θ_0 and the identification of stationary points and a general trend for the complex dependence $\theta_e = \theta_e(\theta_0)$. The existence of two positive and two negative θ_e roots if $\theta_0 \in (-90^\circ, \theta_0^*)$ and one positive and two (eventually three) negative θ_e roots if $\theta_0 \in (\theta_0^*, 90^\circ)$ for a given θ_0 has been mathematically demonstrated. Previous computations of $\theta_e = \theta_e(\theta_0)$ curves associated with specific $S = S(\theta)$ dependences are in very good agreement with this discussion.

The results obtained concerning the quasi-stability of angular points can be easily applied to confirm and explain earlier theoretical and experimental data describing the evolution of various surface microfeatures during ion erosion.

The following quasi-stable intersections having linear trajectories can be distinguished:

(a) surface–surface, plane–surface or plane–plane intersections characterized by random orientations (θ_0^1, θ_0^2) which do not satisfy the quasi-stability condition, leading to the instantaneous initiation of new angular points and finally to the drastic change of the ion eroded microrelief;

(b) surface–surface or plane–surface intersections characterized by special orientations $(\theta_0, \theta_e(\theta_0))$ where θ_0, θ_e are roots of the previously inferred equation for angular point quasi-stability;

(c) plane–plane intersections characterized by a very narrow range of (θ_0, θ_e) orientation pairs, coinciding with the extremum points of $\theta_e = \theta_e(\theta_0)$.

The quasi-stable intersections, mentioned in the two last cases, remain temporarily unique on a single trajectory until some interference with other adjacent edge trajectories occurs.

Although a local and transient stability will be registered in cases (b) and (c), the true space and time stability leading to an infinite reproduction of the initial microprofile could be obtained only for a special topography resulting from an exclusive combination of the quasi-stable intersections mentioned.

The present idealized approach did not consider complex initial topographies and some important secondary effects (thermal diffusion and facetting, redeposition, non-uniform flow, ion reflection). Further work is necessary to clarify the evolution during ion bombardment of a well characterized pre-existing microtopography deliberately obtained on textured surfaces.

References

1. J. P. DUCOMMUN, M. CANTAGREL and M. MOULIN, *J. Mater. Sci.* **10** (1975) 52.
2. G. CARTER, J. S. COLLIGON and M. J. NOBES, *Rad. Effects* **31** (1977) 65.
3. J. P. DUCOMMUN, M. CANTAGREL and M. MARCHAL, *J. Mater. Sci.* **9** (1974) 725.
4. R. SMITH and J. M. WALLS, *Phil. Mag. A* **42** (1980) 235.
5. R. SMITH, T. P. VALKERING and J. M. WALLS, *ibid.* A44 (1981) 879.
6. F. VASILIU and S. FRUNZĂ, *J. Mater. Sci.* **18** (1983) 3562.
7. C. CATANĂ, J. S. COLLIGON and G. CARTER, *ibid.* **7** (1972) 467.
8. T. ISHITANI, M. KATO and R. SHIMIZU, *ibid.* **9** (1974) 505.
9. G. CARTER, M. J. NOBES, K. I. ARSHAK, R. P. WEBB, D. EVANSON, B. D. L. EGHAWARY and J. H. WILLIAMSON, *ibid.* **14** (1979) 728.
10. F. VASILIU and S. FRUNZĂ, *J. Mater. Sci. Lett.* **2** (1983) 249.
11. G. W. LEWIS, G. CARTER, M. J. NOBES and S. A. GRUZ, *Rad. Effects Lett.* **58** (1981) 119.
12. D. J. BARBER, F. C. FRANK, M. MOSS, J. W.

STEEDS and I. S. T. TSONG, *J. Mater. Sci.* 8 (1973) 1030.
13. M. J. NOBES, J. S. COLLIGON and G. CARTER, *ibid.* 4 (1969) 730.
14. G. CARTER, J. S. COLLIGON and M. J. NOBES, *ibid.* 8 (1973) 1473.
15. G. W. LEWIS, M. J. NOBES, G. CARTER and J. L. WHITTON, *Nucl. Instrum. Meth.* 170 (1980) 363.
16. G. CARTER, M. J. NOBES and J. L. WHITTON, *J. Mater. Sci.* 13 (1978) 2725.
17. H. DIMIGEN, H. LUTHJE, H. HUBSCH and U. CONVERTINI, *J. Vac. Sci. Technol.* 13 (1976) 976.
18. G. K. WEHNER, *J. Appl. Phys.* 30 (1959) 1762.
19. B. B. MECKEL, T. NENADOVIC, B. PEROVIC and A. VLAHOV, *J. Mater. Sci.* 10 (1975) 1188.
20. M. J. WITCOMB, *ibid.* 9 (1974) 551.
21. *Idem, ibid.* 11 (1976) 859.
22. F. VASILIU, *Rev. Roum. Phys.* 5 (1977) 523.
23. F. VASILIU and S. FRUNZĂ, *ibid.* 6 (1977) 601.
24. F. VASILIU, *Rad. Effects* 45 (1980) 213.
25. R. KELLY and O. AUCIELLO, *Surface Sci.* 100 (1980) 135.
26. I. A. TEODORESCU and F. VASILIU, *Rad. Effects* 15 (1972) 101.
27. O. AUCIELLO, R. KELLY and R. IRICHIBAR, *ibid.* 46 (1980) 105.
28. O. AUCIELLO and R. KELLY, *ibid.* 66 (1982) 195.
29. J. L. WHITTON, G. CARTER, M. J. NOBES and J. S. WILLIAMS, *ibid.* 32 (1977) 129.
30. G. CARTER, M. J. NOBES, J. L. WHITTON, J. S. WILLIAMS and L. TANOVIC, Proceedings 7th International Conference on Atomic Collisions in Solids, Moscow, 1977, Vol. 2 (Moscow State University Publ. House, 1980) p. 69.
31. J. L. WHITTON, L. TANOVIC and J. S. WILLIAMS, *Appl. Surf. Sci.* 1 (1978) 408.
32. J. L. WHITTON, O. HOLCK, G. CARTER and M. J. NOBES, *Nucl. Instrum. Meth.* 170 (1980) 371.
33. L. T. CHADDERTON, *Rad. Effects* 33 (1977) 129.
34. O. AUCIELLO and R. KELLY, *Rad. Effects Lett.* 43 (1979) 187.
35. P. HAYMANN, *Rev. Metall.* 58 (1961) 73.
36. P. HAYMANN and C. WALDBURGER, "Ionic Bombardment Theory and Applications" (Gordon and Breach, New York, 1964) p. 294.
37. W. HAUFFE, *Phys. Status Solidi (a)* 4 (1971) 111.
38. P. G. GLOERSEN, *J. Vac. Sci. Technol.* 12 (1975) 28.
39. M. CANTAGREL, *Microelectron. Reliab.* 14 (1975) 419.

Received 2 August
and accepted 21 September 1983